



INTERNATIONAL JOURNAL OF ENGINEERING SCIENCES & RESEARCH TECHNOLOGY

Synthesis of $MTiO_3$ (M = Ba, Sr) Nanoparticles in n-butylamine by Following a Solvothermal Route

Chunxia Chai², Xiaoming Shi³, Zhiguang⁴, Yang, Ke Li⁵, Peng Peng*¹

College of Chemistry and Chemical Engineering, Zhoukou Normal University, Zhoukou Henan 466001, PR. China

pengpeng@zknpu.edu.cn

Abstract

Barium titanate ($BaTiO_3$) and strontium titanate ($SrTiO_3$) nanoparticles are prepared in n-butylamine by following a solvothermal route. The as-prepared $BaTiO_3$ and $SrTiO_3$ nanoparticles were characterized by X-ray diffraction (XRD), transmission electron microscopy (TEM), and high resolution transmission electron microscopy (HR-TEM). The results indicate that the as-prepared $BaTiO_3$ are about 20 nm in diameter and $SrTiO_3$ nanoparticles are about 16 nm in diameter. The formation mechanism finally was discussed, and the preliminary results suggest that this synthesis procedure could be developed to a general strategy for the preparation of other perovskite nanoparticles.

Keywords: Barium titanate; Strontium titanate; Nanoparticle; Solvothermal.

Introduction

Perovskite materials, including barium titanate ($BaTiO_3$) and strontium titanate ($SrTiO_3$) are of interest for numerous technical applications, [1] such as solid oxide electronic device, [2] photocatalyst [3]-[7] and dye-sensitized solar cells. [8-9] Furthermore, the rapid development in multilayered ceramic capacitors (MLCCs) requires the size of $MTiO_3$ (M=Ba, Sr) particles to be decreased to tens of nanometers for reduction of capacitor dimension. [10] Perovskites are traditionally prepared by solid state reaction at high temperature. However, the size distribution and morphology of perovskite particles are hard to control. [11] So, the low temperature methods are developed to prepare nanosized $MTiO_3$ (M=Ba, Sr) particles with controllable size distribution and morphology. Recently, various synthesis procedures are reported to prepare perovskite nanoparticles, such as sol-gel, [12] microemulsion-mediated synthesis, [13] thermal decomposition of suitable precursors [14] and solvothermal methods, [15] – [18] and so on. Among them, solvothermal method is used widely in inorganic synthesis due to its moderate condition and tunable medium.

For $MTiO_3$ (M=Ba, Sr), titanium oxide and alkoxy titanate are generally selected as precursors under solvothermal condition and the particle size usually depends on the scale of framework connected by corner-shared TiO_6 octahedra. In general, the

$MTiO_3$ (M=Ba, Sr) size is effected by the relative rates of nuclei formation and crystal growth [19]. It is effective to minimize the size of $MTiO_3$ (M=Ba, Sr) particles when the hydrolysis rate of alkoxy titanate and the subsequential growth rate of crystal are both controlled. In previous work, we have successfully prepared cubic $BaTiO_3$ nanoparticles in n-butanol aqueous solution and the mechanism was promoted to explain the formation of $BaTiO_3$ nanocubes. [20] In this paper, n-butylamine was used as solvent in our experiments, and $BaTiO_3$ and $SrTiO_3$ nanoparticles were conveniently prepared.

Experiment and Characterization

Preparation of samples

Preparation of $MTiO_3$ (M=Ba, Sr) followed a typical experiment approach: 0.006 mol of $Ti(OC_4H_9)_4$ and 0.0072 mol of $M(OH)_2 \cdot 8H_2O$ (M=Ba, Sr) were added into 20 mL of n-butylamine ($NH_2C_4H_9$) with vigorously magnetic stirring for 2 h, and the mixture were transferred to Teflon-lined autoclaves and maintained at different temperature for 24 h. The final white precipitates were filtrated and washed using diluted formic acid, deionized water and ethanol several times in turn. The as-prepared samples were dried for 12 h at 80 °C.

Characterization of samples

Powder X-ray diffraction (XRD) of the samples were measured on a Rigaku D/max 2500 V/PC diffractometer using Cu Ka radiation ($\lambda=1.54056 \text{ \AA}$, 40 kV, 100 mA). Transmission electron microscopy (TEM) images were obtained on Hitachi H-7650, while high resolution TEM (HE-TEM) images were observed on a JEOL 100CX-II PHILIPS-TECNAI G2 F20 (200 kV).

Results and discussion

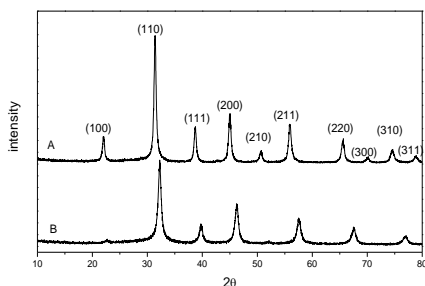


Fig. 1 XRD patterns of BaTiO₃ (A), and SrTiO₃ (B) prepared at 180 °C for 24 h.

In order to investigate the influence of temperature on BaTiO₃ and SrTiO₃, a set of tests are designed to optimize parameters and the results are listed in Table 1. Powder X-ray diffraction (XRD) analysis of the as-prepared materials shows that there is anatase impurity in sample at 140 °C and 160 °C. The pure BaTiO₃ and SrTiO₃ were prepared at 180 °C for 24 h. Fig. 1 shows the XRD patterns of samples of B-1 (Fig. 1A) and S-1 (Fig. 1B), respectively. The peaks of Fig. 1A can be indexed to BaTiO₃ (JCPDS No. 31-0174), and the peaks of Fig. 1B can be indexed to SrTiO₃ (JCPDS No. 73-0661). The anatase impurities were in samples of B-2, S-2, S-3, and S-4 according to Table 1. The anatase ratio in SrTiO₃ products is 6.8%, 4.4%, and 1.5% at 120 °C, 140 °C, and 160 °C, respectively. Furthermore, the anatase ratio in BaTiO₃ products is 2.3% at 160 °C. It suggests that anatase is readily precipitated earlier than MTiO₃ at lower than 180 °C. The phase ratio of anatase decreased at elevated temperatures. That can be well explained according to Venigalla’s work about thermodynamics of Ba-Ti-H₂O system: [21] anatase is preferentially formed at low temperature and in alkaline condition (pH > 7). However, anatase is still thermodynamically metastable and becomes activated enough to react with Ba(OH)₂ in aqueous solution at suitable temperature. So, it is reasonable that only pure MTiO₃ is detected at 180 °C. The average diameter of BaTiO₃ nanoparticles calculated from the 100% intensity diffraction (110) based on Debye-Scherrer equation is about 20 nm, and the

average diameter of SrTiO₃ nanoparticles is about 16 nm.

Table 1. Reaction conditions and the final products of BaTiO₃ and SrTiO₃

Sample	Reaction time (h)	Reaction temperature (°C)	Results ^a
S-1	24	180	Pure SrTiO ₃
S-2	24	160	SrTiO ₃ + 1.5 % anatase
S-3	24	140	SrTiO ₃ + 4.4 % anatase
S-4	24	120	SrTiO ₃ + 6.8 % anatase
B-1	24	180	Pure BaTiO ₃
B-2	24	160	BaTiO ₃ + 2.3 % anatase

a. The phase proportion of anatase in each result was calculated based on peaks area of anatase (101) and MTiO₃ (M=Ba, Sr) (110) diffractions, respectively.

Fig. 2 shows TEM images of BaTiO₃ and SrTiO₃ nanoparticles obtained at 180 °C for 24 h. Fig. 2a and b shows obtained BaTiO₃ samples are uniform size nanoparticles, but slightly aggregated. The magnified images (Fig. 3c) shows that BaTiO₃ nanoparticles are irregularly spherical with diameter of 15-20 nm, which agree with the result of XRD pattern. The TEM images of SrTiO₃ are listed in Fig. 3d-f. Similarly, SrTiO₃ nanoparticles are also irregularly spherical with diameter of 10-15 nm.

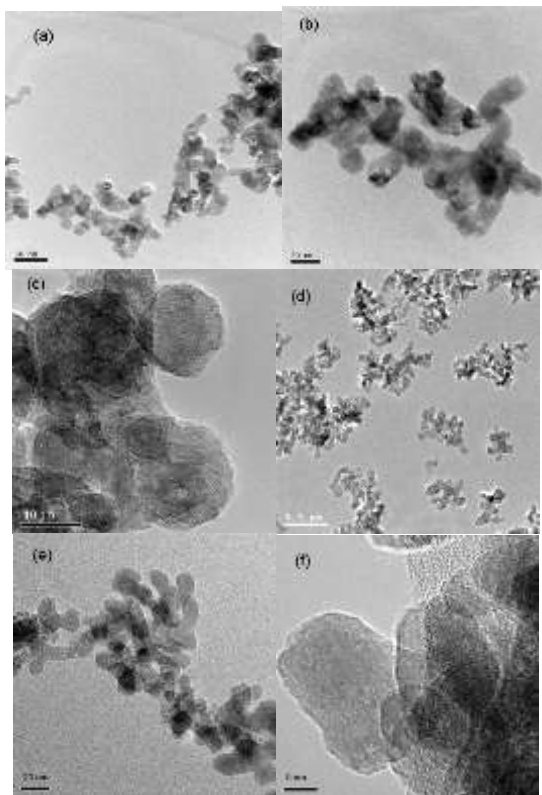
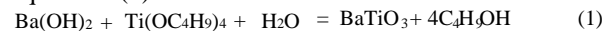


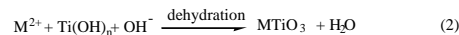
Fig. 2 TEM images at different resolutions of BaTiO₃ (a, b, c) and SrTiO₃ (d, e, f) nanoparticles as-prepared at 180 °C for 24 h.

In order to control the size of particles, the first question needed to consider is decreasing hydrolysis rate of Ti(OC₄H₉)₄. Like other alkoxides, the hydrolysis and condensation of Ti(OC₄H₉)₄ are controlled by two parameters: the concentration of the reactants and the amount of water.[22] Considering that total water needed is just equivalent with precursors in overall reaction according to equations (1):

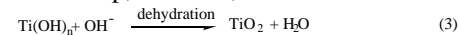


However, there is no additional water except for those existing in precursor of M(OH)₂·8H₂O. The hydrolyzing of Ti(OC₄H₉)₄ is slow at beginning of reaction because only part of crystal water is released from precursor of M(OH)₂·8H₂O at the lower temperature than 180 °C. [23] When the reaction temperature is as high as 180 °C, more crystal water could be released and participate in hydrolysis reaction. [24] This hydrolysis procedure above mentioned is denoted as so-called ‘release-hydrolysis’. In alkaline condition, two routes would be followed in subsequent crystallite growth. Firstly, short corner shared TiO₆ framework is fabricated with M²⁺ inserted, along which step MTiO₃ (M=Ba,

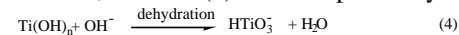
Sr) can be formed. This process can be illustrated by formula:



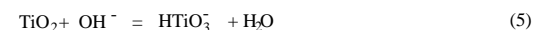
Secondly, only corner or edge shared TiO₆ framework is fabricated with no M²⁺ inserted, along which step, however, TiO₂ is formed:



At higher temperature and in alkaline aqueous solution, reaction (3) can be replaced by reaction (4):



Another probability is consequent reaction by following reaction:



MTiO₃ is consequently generated from species HTiO₃⁻, illustrated by reaction (6)



Fig. 3 (a) and (b) are the HRTEM images of BaTiO₃ and SrTiO₃ nanoparticles obtained at 180 °C for 24 h. Both of images reveals the BaTiO₃ and SrTiO₃ nanoparticles are well crystallinity with interplanar spacing of about 2.84 Å for BaTiO₃, and 2.73 Å for SrTiO₃ respectively. The results correspond to the (110) crystalline planes of both BaTiO₃ and SrTiO₃, suggesting the same growth habit between BaTiO₃ and SrTiO₃ nanoparticles in n-butylamine under solvothermal condition. [25] The solid lines in images show lattice fringes paralleled by crystallite

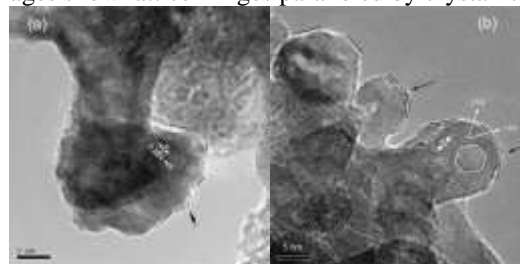


Fig. 3 HRTEM image of (a): BaTiO₃, (b): SrTiO₃ nanoparticles obtained at 180 °C for 24 h, the selected hexagon area in (b) shows a platform of close stack of TiO₆ octahedron. Solid lines in (a) and (b) illustrate fringes of particles and protuberances pointed out by arrows stand out of lattice fringes.

facets. The protuberances pointed out by arrows demonstrate unclosed fringe and crystal growth direction. It is reasonable to assume that the crystallites grow along [110], which suggests TiO₆ octahedrons are preferentially formed in planes (110) and (101) by following a release-hydrolysis procedure. [26] – [27]

As reported previously, the growth of BaTiO₃ nanoparticles under solvothermal conditions is probably attributed to dissolution-crystallization mechanism.[28] – [29] For MTiO₃, the particles nucleate by following reaction (6) and larger crystals

begin to grow at expense of smaller crystals. N-butylamine is adsorbed on the surface of embryos to slow down the ripening process of MTiO_3 , and restrain MTiO_3 to grow. So, the particles of MTiO_3 seem like irregular in TEM images.

Conclusion

In conclusion, we present an effective and facile solvothermal route, following which the well-crystallized MTiO_3 (M=Ba, Sr) nanoparticles are synthesized. The diameter of obtained nanoparticles is about 20 nm for BaTiO_3 and 16 nm for SrTiO_3 . N-butylamine plays an important role of controlling crystallites growth via being adsorbed on the surface of particles. This method is expected to develop other perovskites nanomaterials in further work.



Acknowledgements

The authors would like to thank “Young Teacher Project of Henan Province” (2011GGJS-162).

References

1. A. K. Tagantsev, V. O. Sherman, K. F. Astafiev, J. Venkatesh, and N. Setter, *J. Electroceram.* 11, 5 (2003).
2. L. Pellegrino, I. Pallecchi, D. Marre, E. Bellingeri, and A. S. Siri. *Appl. Phys. Lett.* 81, 3849 (2002).
3. K. Domen, S. Naito, T. Onishi, K. Tamaru, and M. Soma. *J. Phys. Chem.* 86, 3657 (1982).
4. M. Miyauchi, A. Nakajima, A. Fujishima, K. Hashimoto, and T. Watanabe. *Chem. Mater.* 12, 3 (2000).
5. H. Kato, and A. Kudo, *J. Phys. Chem. B.* 106, 5029 (2002).
6. R. Kouta, T. Ishii, H. Kato, and A. Kudo. *J. Phys. Chem. B.* 108, 8992 (2004).
7. M. Miyauchi, M. Takashio, H. Tobimatsu. *Langmuir.* 20, 232 (2004).
8. S. Burnside, J. E. Moser, K. Brooks, M. Grätzel, and D. Cahen. *J. Phys. Chem. B.* 103, 9328 (1999).
9. F. Lenzmann, J. Krueger, S. Burnside, K. Brooks, M. Grätzel, D. Gal, S. Rühle, and D. Cahen. *J. Phys. Chem. B.* 105, 6347 (2001).
10. W. K. Zhang, X. L. Tong, H. Huang, Y. P. Gan, N. Huang, and J. Chin. *Nonferr. Metal. Soc.* 15, 643 (2005).
11. I. Maclaren, and C. B. Ponton. *J. Eur. Ceram. Soc.* 20, 1267 (2000).
12. Y. F. Li, and Q. Y. Lai, *Chin. J. Inorg. Chem.* 21, 915 (2005).
13. I. W. Lenggoro, C. Panatarani, and K. Okuyama, *Mater. Sci. Eng. B.* 113, 60 (2004).
14. S. C. Zhang, J. X. Liu, Y. X. Han, B. C. Chen, and X. G. Li, *Mater. Sci. Eng. B.* 110, 11 (2004).
15. D. R. Chen, X. L. Jiao, and M. S. Zhang, *J. Euroceram. Soc.* 20, 1261 (2000).
16. S. C. Zhang, Y. X. Han, B. C. Chen, and X. P. Song, *Mater. Lett.* 51, 368 (2001).
17. S. Burnside, J. E. Moser, K. Brooks, M. Grätzel, and D. Cahen, *J. Phys. Chem. B.* 103, 9328 (1999).
18. Y. Jing, S. Jin, Y. Z. Jia, J. D. Han, and J. H. Sun, *J. Mater. Sci.* 40, 6315 (2005).
19. J. A. Dirksen, and T. A. Ring, *Chem. Eng. Sci.* 46, 2389 (1991).
20. Q. Liu, Z. Y. Yan, G. X. Sun, and W. J. Zheng, *Chem. Lett.* 36, 458 (2007).
21. S. Venigalla, J. H. Adair, *Chem. Mater.* 11, 589 (1999).
22. A. C. Pierre, *Introduction to Sol-Gel Processing*, Kluwer Academic Publishers, Dordrecht. p. 68 (1998).
23. A. Friedrich, M. Kunz, and R. Miletich, *Phys. Rev. B.* 66, 214103 1-8 (2002).
24. J. G. Giuntini, W. Granier, J. V. Zanchetta, and A. Taha, *J. Mater. Sci. Lett.* 9, 1383 (1990).
25. B. C. Russell, and M. R. Castell, *Phys. Rev. B.* 75, 155433 1-7 (2006).
26. V. Werner, and H. Bauer, *Acta Cryst.* 9, 515 (1956).
27. P. Jone, and A. Hockey, *Trans. Faraday Soc.* 67, 2679 (1971).
28. J. Moon, E. Suvaci, A. Morrone, S. A. Costantino, and J. H. Adair, *J. Eur. Ceram. Soc.* 23, 2153 (2003).
29. A. Testino, M. T. Buscaglia, V. Buscaglia, M. Viviani, C. Bottino, and P. Nanni, *Chem. Mater.* 16, 1536 (2004).

Author Bibliography

	<p>Chunxia Chai Accept her M. S of Henan Normal University in 2009, and has been working in Zhoukou Normal University as a lecture since 2002. Email: ccxy66@126.com</p>
	<p>Peng Peng Accept his Ph. D. of Nankai University in 2009, and has been working in Zhoukou Normal University as a assistant professor since 2010. Email: author@xxx.xxx</p>